Journal of Molecular and Cellular Cardiology 74 (2014) 260–273

Contents lists available at ScienceDirect

Journal of Molecular and Cellular Cardiology

journal homepage: www.elsevier.com/locate/yjmcc

Original article

High-mobility group box 1 (HMGB1) impaired cardiac excitation–contraction coupling by enhancing the sarcoplasmic reticulum (SR) Ca^{2+} leak through TLR4–ROS signaling in cardiomyocytes

Cuicui Zhang [b,1], Miaohua Mo [a,1], Wenwen Ding [b], Wenjuan Liu [a], Dewen Yan [c], Jianxin Deng [b], Xinping Luo [a], Jie Liu [a,b,*]

[a] Department of Pathophysiology, School of Medicine, Shenzhen University, Shenzhen, China
[b] Department of Pathophysiology, Key Laboratory for Shock and Microcirculation Research, Southern Medical University, Guangzhou, China
[c] Department of Endocrinology, The First Affiliated Hospital of Shenzhen University, Shenzhen, China

ARTICLE INFO

Article history:
Received 25 March 2014
Received in revised form 4 May 2014
Accepted 8 June 2014
Available online 14 June 2014

Keywords:
HMGB1
Sarcoplasmic reticulum (SR) Ca^{2+} leak
SR Ca^{2+} content
Ca^{2+} transient
Toll-like receptor (TLR) 4
Reactive oxygen species (ROS)

ABSTRACT

High-mobility group box 1 (HMGB1) is a proinflammatory mediator playing an important role in the pathogenesis of cardiac dysfunction in many diseases. In this study, we explored the effects of HMGB1 on Ca^{2+} handling and cellular contractility in cardiomyocytes to seek for the mechanisms underlying HMGB1-induced cardiac dysfunction. Our results show that HMGB1 increased the frequency of Ca^{2+} sparks, reduced the sarcoplasmic reticulum (SR) Ca^{2+} content, and decreased the amplitude of systolic Ca^{2+} transient and myocyte contractility in dose-dependent manners in adult rat ventricular myocytes. Inhibiting high-frequent Ca^{2+} sparks with tetracaine largely inhibited the alterations of SR load and Ca^{2+} transient. Blocking Toll-like receptor 4 (TLR4) with TAK-242 or knockdown of TLR4 by RNA interference remarkably inhibited HMGB1 induced high-frequent Ca^{2+} sparks and restored the SR Ca^{2+} content. Concomitantly, the amplitude of systolic Ca^{2+} transient and myocyte contractility had significantly increased. Furthermore, HMGB1 increased the level of intracellular reactive oxygen species (ROS) and consequently enhanced oxidative stress and CaMKII-activated phosphorylation (pSer2814) in ryanodine receptor 2 (RyR2). TAK-242 pretreatment significantly decreased intracellular ROS levels and oxidative stress and hyperphosphorylation in RyR2, similar to the effects of antioxidant MnTBAP. Consistently, MnTBAP normalized HMGB1-impaired Ca^{2+} handling and myocyte contractility. Taken together, our findings suggest that HMGB1 enhances Ca^{2+} spark-mediated SR Ca^{2+} leak through TLR4–ROS signaling pathway, which causes partial depletion of SR Ca^{2+} content and hence decreases systolic Ca^{2+} transient and myocyte contractility. Prevention of SR Ca^{2+} leak may be an effective therapeutic strategy for the treatment of cardiac dysfunction related to HMGB1 overproduction.

1. Introduction

Inflammatory response and cytokine elaboration are integral components of the host response to multiple pathological stimulations and play a particularly active role in cardiac injury [1,2]. Numerous myocardial cytokines including TNF-α, IL-1, IL-6 and IL-10, have been demonstrated to severely impair cardiac function [3–5]. Recently, another inflammatory cytokine, high-mobility group box 1 (HMGB1) has aroused much attention for its important role in the pathogenesis of cardiac dysfunction in many diseases, such as ischemic heart diseases, sepsis, and diabetic cardiomyopathy [6–9]. HMGB1 is a nuclear factor released passively by necrotic cells and actively by activated immune cells. Once released into the extracellular milieu, HMGB1 activates inflammatory responses, serving as a late mediator of systemic inflammation [10]. It has been demonstrated that the serum HMGB1 level was significantly increased in patients with ST-elevation myocardial infarction (MI). Strikingly, the serum HMGB1 level was associated with the severity of heart injury. A high peak serum HMGB1 level was associated with pump failure, cardiac rupture, and in-hospital cardiac death in patients with MI [11]. In addition, the plasma concentration of HMGB1 was correlated with the degree of organ dysfunction during

Abbreviations: HMGB1, high-mobility group box 1; MI, myocardial infarction; HF, heart failure; RyR, ryanodine receptor; EC, excitation–contraction coupling; SR, sarcoplasmic reticulum; CICR, Ca^{2+}-induced Ca^{2+} release; ROS, reactive oxygen species; TLR4, Toll-like receptor 4; ARVMs, adult rat ventricular myocytes; NRVMs, neonatal rat ventricular myocytes; DCFDA, 5-(and-6) chloromethyl-dichlorodihydrofluoroscein diacetate; mBB, monobromobimane; AP, action potential; FWHM, full width at half-maximum; FDHM, full duration at half-maximum; NCX, Na^{+}–Ca^{2+} exchanger; CaMKII, Ca^{2+}/calmodulin dependent protein kinase.

* Corresponding author at: Department of Pathophysiology, School of Medicine, Shenzhen University, Shenzhen 518060, China. Tel.: +86 755 8667 1912; fax: +86 755 8667 1906.
E-mail address: ljljz@yahoo.com (J. Liu).
[1] These authors contributed equally to this work.

http://dx.doi.org/10.1016/j.yjmcc.2014.06.003
0022-2828/

septic shock [12] and the severity of heart failure (HF) in both diabetic and non-diabetic patients [13]. Passive immunization with either neutralizing anti-HMGB1 antibodies or HMGB1-specific blockage via box A treatment prevented cardiac dysfunction in mice with ischemia–reperfusion injury [14], sepsis [15], and diabetic cardiomyopathy [8]. All the evidence supports the importance of HMGB1 in the pathogenesis of cardiac dysfunction in these diseases.

Of note, despite the deleterious effects, HMGB1 has long-term beneficial effects due to the induction of myocardial regeneration and attenuation of left ventricular remodeling, especially in ischemic heart diseases [11,16]. Thus, extracellular HMGB1 may activate signals that promote either cardiac adaptation/protection or maladaptive responses. In this consideration, elucidating the mechanisms which specifically induce the deleterious effects of HMGB1 is of particular importance for the design of effective therapeutic strategy preventing the deleterious effects of HMGB1 without affecting its cardioprotective activity.

The cardiac ryanodine receptor (RyR2) plays an essential role in cardiac excitation–contraction coupling (EC coupling) by gating Ca^{2+} release from the sarcoplasmic reticulum (SR) via the Ca^{2+}-induced Ca^{2+} release (CICR) mechanism [17,18]. There is evidence that the SR leaks calcium through RyR2 even in the absence of stimulation at resting state, which may have a protective role against an excessive increase of SR Ca^{2+} content [19]. However, if RyR2 becomes excessively active, it will reduce SR Ca^{2+} content by enhancing diastolic SR Ca^{2+} leak, resulting in a decrease of systolic Ca^{2+} transient and hence contractile dysfunction in cardiomyocytes [20–22]. Furthermore, enhancement of SR Ca^{2+} leak during diastole could initiate Ca^{2+} waves through CICR mechanism and trigger cardiac arrhythmias [23,24]. Evidence from various models of heart failure (HF) suggests that cardiac RyR2s became excessively active i.e., "leaky", which plays an important role in promoting the pathogenesis of HF [20,22,25]. Recently, it has been shown that inflammatory factor TNF-α caused SR Ca^{2+} leak, which contributes to arrhythmia, cardiac infarction and myocardial remodeling in cardiac ischemia–reperfusion injury [26].

It is well recognized that RyR2 acts as a cellular redox sensor due to the rich free thiol groups in its structure [27,28]. In particular, the oxidation of its cysteine groups facilitates RyR opening and SR Ca^{2+} leak. Yano et al. has demonstrated that oxidative stress of RyR2 produced SR Ca^{2+} leak by destabilizing the interdomain interactions within RyR2, which accounts for SR Ca^{2+} leak in HF [25]. Research from Gyorke's lab has also shown that redox modification of RyR2s increased the open probability of the Ca^{2+} releasing channels, leading to SR Ca^{2+} leak in chronic HF [20]. Furthermore, intracellular oxidative stress has been shown to activate Ca^{2+}/calmodulin dependent protein kinase II (CaMKII) by oxidizing the enzyme and consequently increased RyR activity by phosphorylation of RyR at Ser2814 [29,30].

It has been suggested that HMGB1 causes TLR4-dependent activation of NAD(P)H oxidase as well as increased reactive oxygen species (ROS) production through both MyD88–IRAK4–p38 MAPK and MyD88–IRAK4–Akt signaling pathways [31,32]. We thus proposed that HMGB1 induces SR Ca^{2+} leak and hence negative inotropic effect in cardiomyocytes. To test this hypothesis, we investigated the effects of HMGB1 on Ca^{2+} handling and myocyte contractility in isolated adult rat ventricular myocytes. The results show that HMGB1 enhanced Ca^{2+} spark-mediated SR leak by activation of TLR4/ROS signaling pathway. The enhancement of SR leak decreased SR Ca^{2+} content, which consequently diminished systolic Ca^{2+} transient and impaired cardiac contractile function.

2. Materials and methods

2.1. Isolation of adult rat ventricular myocytes

Adult Sprague–Dawley rats of either sex, weighing 200 to 250 g from animal center of Southern Medical University were used throughout the study. All animal experiments were performed in accordance with ethical standards as formulated in the Guide for the Care and Use of Laboratory Animals published by the US National Institutes of Health (NIH Publication no. 85-23, revised 1996) and approved by Institutional Animal Care and Use Committee of Shenzhen University. Adult rat ventricular myocytes (ARVMs) were isolated as described previously [33]. In brief, after deep anesthesia with trichloroacetaldehyde monohydrate (0.5 g/kg, i.p.), the heart was removed and cleaned and flushed with Ca^{2+}-free Tyrode solution consisting of (in mM) 137 NaCl, 5.4 KCl, 1.2 $MgCl_2$, 1.2 NaH_2PO_4, 10 glucose, and 20 HEPES (pH 7.4, adjusted with NaOH), and perfused using a Langendorff apparatus. 5 min after perfusion at 37 °C, the solution was switched to the enzyme solution with 0.5 mg/ml collagenase (Worthington, Type II) and 0.06 mg/ml protease (Sigma, Type XIV) for 15 min. After that, the heart was minced into small chunks and single cells were shaken loose from the heart tissue and stored in HEPES-buffered external solution containing (mM): 137 NaCl, 5.4 KCl, 1 $CaCl_2$, 1.2 $MgCl_2$, 1.2 NaH_2PO_4, 20 glucose and 20 HEPES (pH 7.4). The isolated cells were used within 6 h after isolation.

2.2. Culture of neonatal rat ventricular myocytes

Neonatal rat ventricular myocytes (NRVMs) were isolated from 2-day-old Sprague–Dawley rats and cultured as previously described [34]. In brief, ventricles were obtained following decapitation and immersed in PBS and minced with scissors. The small pieces of ventricular tissue were digested with 0.25% Trypsin–EDTA in PBS at 37 °C. The isolated cells were put in fetal bovine serum (FBS) and pelleted by centrifugation at 1000 rpm for 5 min. The pelleted cells were resuspended in DMEM containing 10% FBS, 1% penicillin–streptomycin and then preplated for 30 min at 37 °C to allow fibroblasts to adhere to the plate. The un-adhered cells were pelleted again and resuspended in DMEM containing 10% FBS, 1% penicillin–streptomycin and bromodeoxyuridine (1:100, to inhibit fibroblast growth), which were finally plated at a concentration of about 1 million cells per 35 mm plate.

2.3. siRNA knockdown of TLR4

The oligonucleotide sequences used for the TLR4 RNA interference (TLR4-shRNA) were as follows: forward, GGAUCAGAAUCUCA GCAAATT; reverse, UUUGCUGAGAUUCUGAUCCTT. Scrambled shRNA (Ctrl-shRNA) was used as a control. The cultured NRVMs were transfected with 0.3 μg TLR4-shRNA or Ctrl-shRNA per 2.5 × 10^5 cells seeded in a 35 mm petri-dish using HiPerFect Transfection Reagent (QIAGEN, USA) according to the manufacturer's instructions. The cells were cultured for 48 h before performing the experiments.

2.4. Ca^{2+} spark and Ca^{2+} transient detection and contraction measurement

Isolated cardiomyocytes loaded with Ca^{2+} indicator fluo-4 AM (5 μmol/l, for 8 min) (Invitrogen) were placed in a recording chamber. Ca^{2+} sparks and transients were recorded as previously reported [21]. For Ca^{2+} spark recording, confocal line-scan imaging was carried out in resting cells at 488 nm excitation and 505 nm collection with a Zeiss 710 inverted confocal microscope (Carl Zeiss, Oberkochen, Germany) with 40× oil immersion lens (NA 1.3). Line-scan images were acquired at a sampling rate of 3.84 ms per line, along the longitudinal axis of the cell. For the detection of systolic Ca^{2+} transient, after the cells were stimulated with field stimulation (1 Hz) to reach a steady state, confocal line-scan imaging was performed with the same confocal parameters used for Ca^{2+} spark recording under field stimulation (1 Hz). Myocyte contraction was measured by detecting the length of two edges of the cell along with the time of stimulation. Myocytes were superfused with HEPES-buffered external solution during the experiment.

2.5. Measurement of SR Ca^{2+} load

Short puffs of caffeine (20 mmol/l) were applied to completely empty the SR, following a train of 1 Hz field stimulation to achieve steady-state SR Ca^{2+} loading in ARVMs. SR Ca^{2+} content was assessed by detecting the amplitude of caffeine-elicited Ca^{2+} transient. Cells were superfused with HEPES-buffered external solution.

2.6. Measurement of reactive oxygen species (ROS) in cardiomyocytes

The intracellular ROS level was detected as described previously [20,35]. In brief, isolated cardiomyocytes were loaded with 10 μM 5-(and-6) chloromethyl-dichlorodihydrofluoroscein diacetate (DCFDA, Invitrogen) for 30 min at room temperature, followed by 15 min for de-esterification. Frame fluorescence images (excitation at 488 nm and emission at 505–530 nm, laser intensity 4%, 6.6 s/frame) were acquired with a Zeiss 710 inverted confocal microscope with 20× lens. Since DCFDA is light sensitive and oxidized progressively, we used the same scanning parameters for all the related experiments. Each experiment was performed within 5 min.

2.7. Oxidative stress level in RyR2

The content of the free thiols, i.e., the number of reduced cysteines, in RyR2 in cardiomyocytes was determined with the monobromobimane (mBB, Calbiochem, San Diego, California) fluorescence technique [20,25]. Heavy SR vesicles were prepared from different groups of cells under non-reducing conditions. Samples were incubated with 400 mol/l mBB for 1 h in the dark at room temperature. Then, proteins were acetone precipitated and subjected to SDS-PAGE (in a 6% polyacrylamide gel). The mBB fluorescence was measured using BIO-PEOFLL (Vilber Lourmat Biotechnology, French; excitation 365 nm and emission 400–600 nm). Images were acquired and analyzed using Biocapt software. After that, the same gel was stained with Coomassie Blue. The mBB fluorescence in the RyR2 (~560 kDa) was normalized by protein abundance of RyR2 determined by Coomassie Blue staining of the same gel, which was defined as the relative content of free thiols in the RyR2.

2.8. Western blotting

Total cellular extracts from ARVMs were lysed in Laemmli buffer. Equal amounts of proteins were loaded, separated on 3% to 12% SDS-PAGE before being transferred to polyvinylidene difluoride (PVDF) membranes and then probed with primary antibody: Anti-RyR2 (1:200, Alomone), anti-RyR2-pS2814 (1:2000, Badrilla), anti-CaMKII (1:1000, Santa Cruz), or anti-oxidized CaMKII (1:1000, Gene Tex), followed by horseradish peroxidase (HRP)-conjugated secondary antibody (Santa Cruz) according to a previous study [29]. Bound antibodies were visualized using the enhanced chemiluminescence (ECL) detection kit (Invitrogen). Equal loading was confirmed by immunoblotting for β-actin and subjected to SDS-PAGE in an identical manner.

2.9. Recording of L-type Ca^{2+} current ($I_{Ca,L}$)

$I_{Ca,L}$ was recorded in cardiac ventricular myocytes under whole-cell recording mode with an Axopatch 200B patch clamp amplifier (Axon Instruments, Foster City, CA), as described previously [36]. Bath solution contained (mmol/l): NaCl 137, KCl 5.4, $CaCl_2$ 1.0, $MgCl_2$ 1.2, NaH_2PO_4 1.2, HEPES 20, glucose 10, and 0.02 TTX (pH 7.4). Pipette solution contained (mmol/l): CsCl 120, MgATP 5, HEPES 10, TEA-Cl 20, $MgCl_2$ 1, and EGTA 5, adjusted pH to 7.2 with CsOH. When filled with the pipette solution, pipettes had resistance ranging between 3 and 5 MΩ. The junctional potential was corrected when pipette tip entered the bath solution. After the cell membrane was broken by application of additional suction, cell capacitance and series resistance were electrically compensated. The myocytes were equilibrated for 5 min with the internal solution before data were collected. $I_{Ca,L}$ was elicited by a series of depolarization pulses ranging from −40 to 60 mV for 250 ms from a holding potential of −55 mV at 10-second intervals. Cells showing continuous current run-down (>5%) were excluded from the analysis.

2.10. Image processing and data analysis

Image processing was performed using IDL 6.0 software. Automated detection and analysis of Ca^{2+} sparks were performed using the computer algorithm developed by Cheng et al. [37]. Data were expressed as mean ± SE. One-way or two-way ANOVA and Student–Newman–Keuls multiple-comparison test were applied for statistical analysis. $p < 0.05$ was considered statistically significant.

3. Results

3.1. HMGB1 dose-dependently increased the frequency of Ca^{2+} sparks in cardiomyocytes

Ca^{2+} sparks as the elementary Ca^{2+} release events reflect RyR activities and many features of SR function in intact cells. To investigate whether HMGB1 regulates RyR activity and SR function, we measured the rate and characteristics of Ca^{2+} spark in isolated adult rat ventricular myocytes (ARVMs). The cells were incubated with HMGB1 (50–200 ng/ml) for 30 min before the experiments. We found that HMGB1 dose-dependently increased the rate of Ca^{2+} sparks (Figs. 1A, B). The average frequency of Ca^{2+} spark was 1.5 ± 0.1 Hz/100 μm scanline in control (735 sparks in 112 cells). HMGB1 at the concentration of 50 ng/ml had no significant effect on the frequency of Ca^{2+} sparks (1.7 ± 0.1 Hz/100 μm scanline, n = 546 sparks in 71 cells, $p > 0.05$). The rate of Ca^{2+} spark was significantly increased to 1.56 fold of control by 100 ng/ml HMGB1 (2.3 ± 0.2 Hz/100 μm scanline, n = 808 sparks in 79 cells, $p < 0.01$ vs. control and 50 ng/ml HMGB1), which was further increased to 2.1-fold of control by 200 ng/ml HMGB1 (3.1 ± 0.2 Hz/100 μm scanline, n = 976 sparks in 71 cells, $p < 0.01$ vs. control and 100 ng/ml HMGB1). Meanwhile, we found that HMGB1 slightly decreased the amplitude and the full width at half-maximum (FWHM) of Ca^{2+} sparks, which were also in a dose-dependent manner (Figs. 1C, D). The kinetics of Ca^{2+} sparks indexed by the full duration at half-maximum (FDHM) was unaltered by HMGB1 treatment (Fig. 1E).

3.2. HMGB1 decreased SR Ca^{2+} content

There is a tight interaction between SR Ca^{2+} content and the occurrence of Ca^{2+} sparks. On one hand, the SR Ca^{2+} content determines the frequency of Ca^{2+} sparks. An increase in SR Ca^{2+} content enhances Ca^{2+} spark-mediated SR leak which facilitates restoration of SR load to normal level. On the other hand, the rate of Ca^{2+} sparks determines SR Ca^{2+} content. The abnormal increase of Ca^{2+} spark rate enhances SR Ca^{2+} leak, causing depletion of SR Ca^{2+} content. We thus examined SR Ca^{2+} content in response to HMGB1 stimulation. Figs. 2A and B show that short puffs of 20 mM caffeine induced Ca^{2+} transients which reflect SR Ca^{2+} content. The average amplitude of Ca^{2+} transients indexed by ΔF / F0 in control was 6.1 ± 0.2 (n = 18). HMGB1 dose-dependently decreased SR Ca^{2+} content (Figs. 2A–C). The SR load was significantly decreased by 22% by 100 ng/ml HMGB1 (4.8 ± 0.1, n = 33, $p < 0.01$ vs. control). 200 ng/ml HMGB1 further decreased the SR Ca^{2+} content (3.7 ± 0.1, n = 43) by 39% ($p < 0.01$ vs. 100 ng/ml HMGB1). HMGB1 at the concentrations tested had no significant effects on

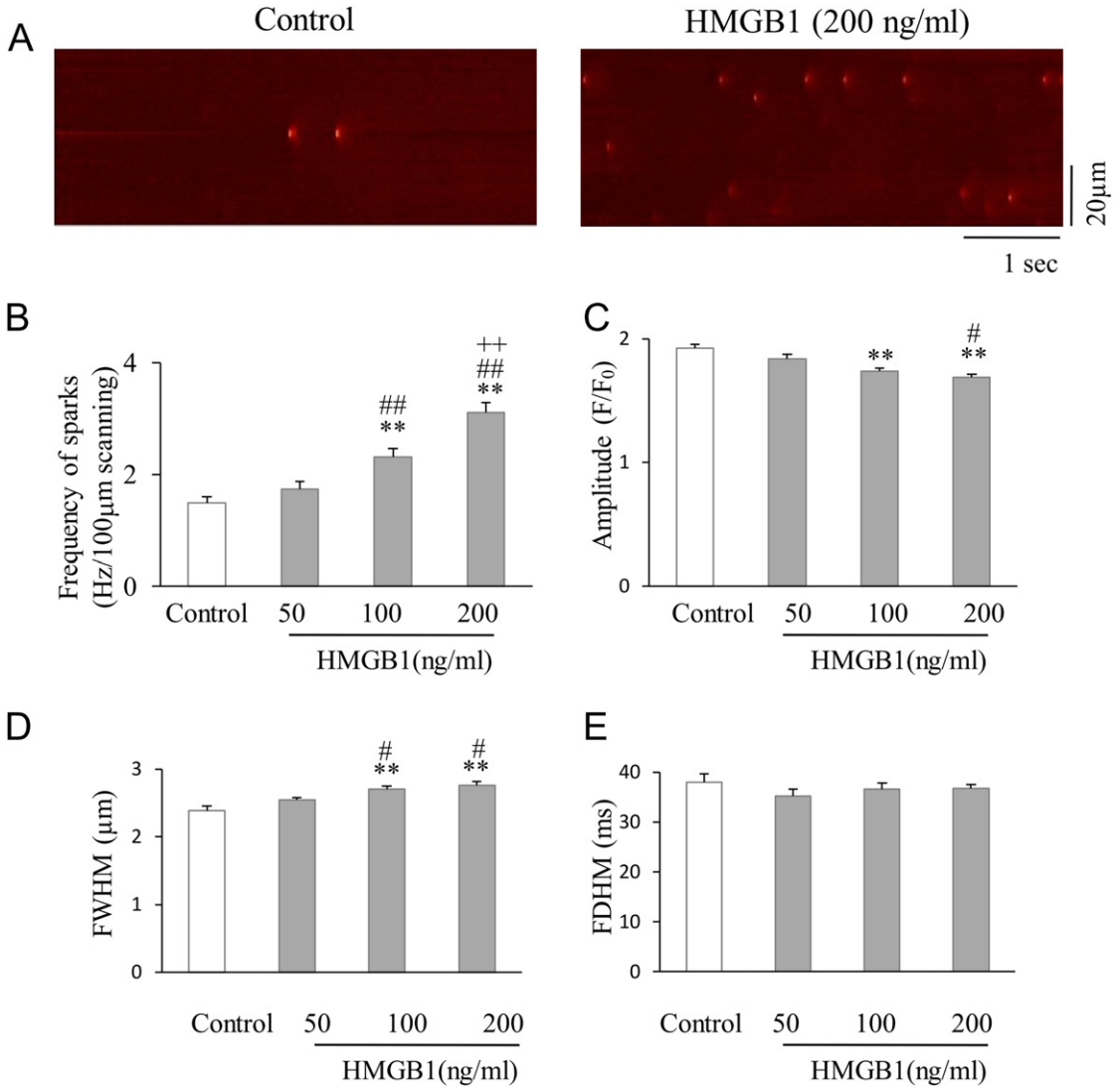

Fig. 1. HMGB1 dose-dependently increased Ca^{2+} sparks in cardiomyocytes. A, representative Ca^{2+} spark images in control and HMGB1 (200 ng/ml)-treated cells. B, average of the frequency of Ca^{2+} sparks in control and 50–200 ng/ml HMGB1-treated cells. C–E, statistics of the amplitude (F / F0, C), full duration at half maximum (FDHM, D) and full width at half maximum (FWHM, E) of Ca^{2+} sparks in control and HMGB1 groups. $^{**}p < 0.01$ vs. control; $^{\#}p < 0.05$, $^{\#\#}p < 0.01$ vs. 50 ng/ml HMGB1; $^{+}p < 0.05$, $^{++}p < 0.01$ vs. 100 ng/ml HMGB1.

the kinetics of caffeine-elicited Ca^{2+} transient indexed by the time to peak and half time of decay (T_{50}, Figs. 2D, E). Collectively, the results suggest that the alteration of SR Ca^{2+} content is the result, rather than the cause of high-frequent Ca^{2+} spark-mediated SR leak under the treatment of HMGB1. Furthermore, the evidence that Ca^{2+} spark increased under reduced SR Ca^{2+} content indicates that RyRs become hyperactive by HMGB1 stimulation.

3.3. HMGB1 decreased systolic Ca^{2+} transient and cell shortening in cardiac myocytes

The SR is the major source of intracellular Ca^{2+} increase leading to myocyte contraction. With the reduction of SR Ca^{2+} content, HMGB1 would decrease systolic Ca^{2+} transient and myocyte contractility. We thus examined AP-elicited Ca^{2+} transient and cell shortening with 1 Hz field stimulation in ARVMs under the treatment of HMGB1. In control cells, the average amplitude of Ca^{2+} transient (indexed by ΔF / F0) was 5.2 ± 0.1, and cellular contractility indexed by the percentage of maximum cell shortening was 10.3 ± 0.2% (Figs. 3A–C). Parallel to the dose-dependent reduction of SR Ca^{2+} content, HMGB1 dose-dependently decreased the cellular contractility and the amplitude of Ca^{2+} transient (Figs. 3A–C). The amplitude of AP-elicited Ca^{2+} transient was decreased by 27% ($p < 0.01$ vs. control) and 39% ($p < 0.01$ vs. control and 100 ng/ml HMGB1), while the cell shortening was decreased by 31% ($p < 0.01$ vs. control) and 43% ($p < 0.01$ vs. control and 100 ng/ml HMGB1), respectively, by 100 and 200 ng/ml HMGB1 treatment. 50 ng/ml HMGB1 had no significant effect on Ca^{2+} transient and myocyte contractility ($p > 0.05$). The rise time was unaltered (Fig. 3D), suggesting that the synchrony of Ca^{2+} release was uncompromised by HMGB1 stimulation. The half time decay of Ca^{2+} transient (T_{50}) was slightly but significantly increased by 100 and 200 ng/ml HMGB1 ($p < 0.01$ vs. control, Fig. 3E). Our previous study demonstrated that HMGB1 prolonged action potential duration (APD) by decreasing transient outward current (I_{to}) [34]. The increase in T_{50} of Ca^{2+} transient might be related to APD prolongation.

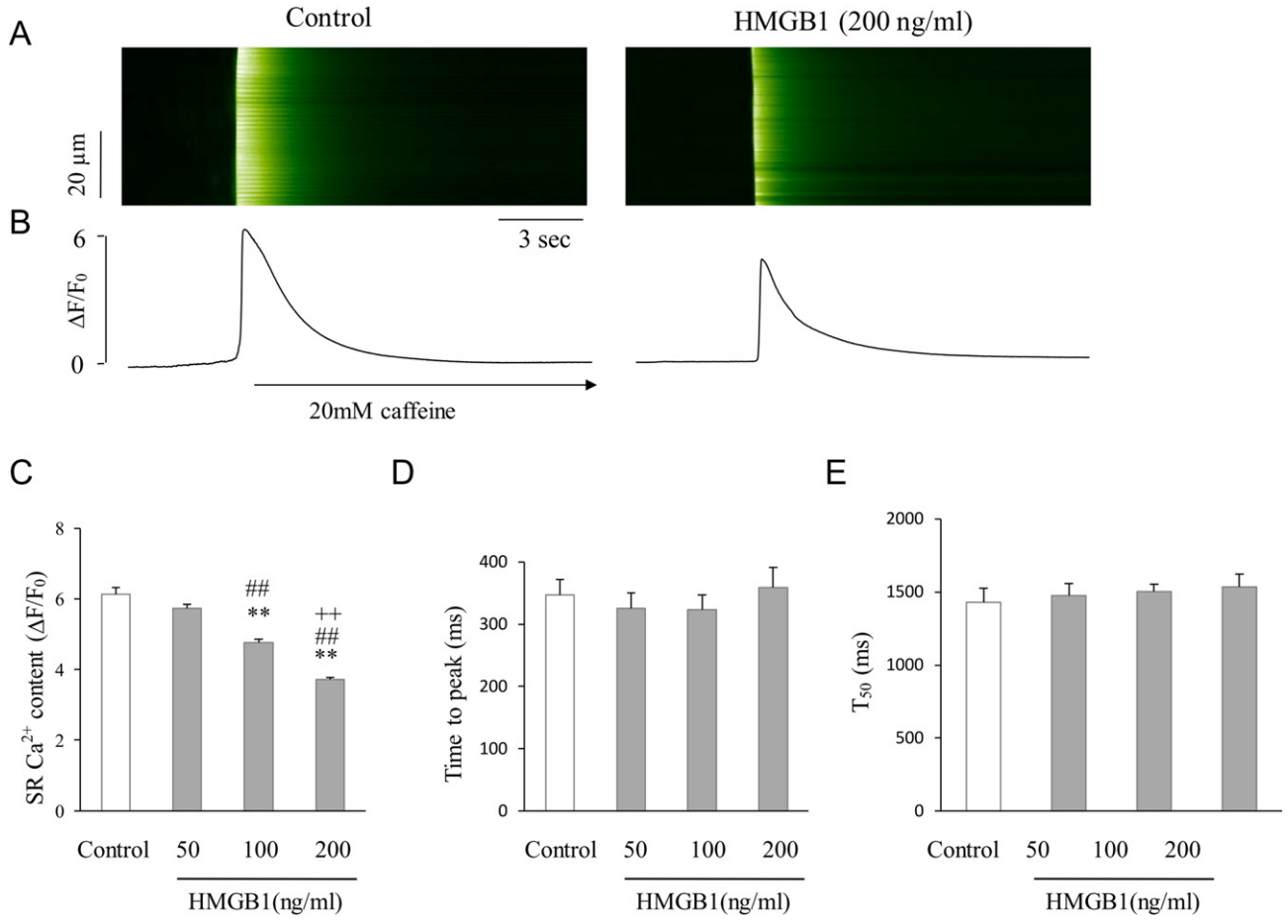

Fig. 2. HMGB1 partially depleted SR Ca^{2+} content in cardiomyocytes. A, B, representative line scan images of Ca^{2+} transient (A) along with the spatial average (B) under the stimulation of 20 mM caffeine in control and HMGB1 (200 ng/ml)-treated cells. C, average of the amplitude of caffeine-induced Ca^{2+} transient in control and different doses of HMGB1 treated groups. D, E, statistics of the time to peak (D) and half-time of decay (T_{50}, E) of caffeine-elicited Ca^{2+} transient. $^{**}p < 0.01$ vs. control; $^{\#\#}p < 0.01$ vs. 50 ng/ml HMGB1; $^{++}p < 0.01$ vs. 100 ng/ml HMGB1.

3.4. Effects of tetracaine on HMGB1 regulation of Ca^{2+} handling and myocyte contractility

To verify the causal relationship between the reduction of SR Ca^{2+} content and the decrease of Ca^{2+} transient, we inhibited Ca^{2+} spark-mediated SR leak with relatively low concentrations of tetracaine which has been shown to block RyR activity without affecting L-type Ca^{2+} current [38]. Tetracaine (25–100 μM) was added 10 min before HMGB1 (200 ng/ml) was applied. The result shows that tetracaine had no significant effect on Ca^{2+} sparks, SR Ca^{2+} content, the amplitude of systolic Ca^{2+} transient and cell shortening in control cells, consistent with previous reports [39,40]. However, tetracaine decreased the frequency of Ca^{2+} sparks increased by HMGB1 in a dose-dependent manner (Fig. 4A). The frequency of Ca^{2+} sparks under HMGB1 stimulation was even lower than normal with the pretreatment of 100 μM tetracaine. Accordingly, HMGB1-depleted SR Ca^{2+} content was dose-dependently increased by tetracaine (Fig. 4B). 25 μM tetracaine restored SR load decreased by HMGB1 by 69%, while 50 and 100 μM tetracaine completely restored SR load. HMGB1-induced decrease of the amplitude of Ca^{2+} transient and cellular shortening were significantly increased by pretreatment with 25 μM tetracaine (increased by 37% and 35%, respectively), 50 μM tetracaine (increased by 60% and 68%, respectively) and 100 μM tetracaine (increased by 55% and 61%, respectively) (Figs. 4C, D). The results indicate that Ca^{2+} spark-mediated SR leak is an important but not the only reason for HMGB1-induced suppression of systolic Ca^{2+} transient and myocyte contractility.

3.5. Roles of Toll-like receptor 4 in HMGB1 regulation of Ca^{2+} handling and myocyte contractility

Toll-like receptor 4 (TLR4) is one of the major receptors for extracellular HMGB1 [32,41,42]. HMGB1–TLR4 interaction is responsible for many of the pathological consequences of HMGB1 [32,42]. Therefore, we tested the effects of HMGB1 on Ca^{2+} handling and cardiac contractility with TLR4 specific inhibitor TAK-242. The results show that pretreatment of the cells with 0.5–2 μM TAK-242 for 30 min had no significant effect on the frequency of Ca^{2+} sparks in control (Fig. 5A). However, TAK-242 pretreatment significantly decreased the frequency of Ca^{2+} sparks increased by HMGB1 (200 ng/ml) in a dose-dependent manner ($p < 0.05$ at 100 ng/ml, $p < 0.01$ at 200 ng/ml vs. HMGB1, Figs. 5A, B). The decrease of the amplitude of Ca^{2+} sparks by HMGB1 was also attenuated by TAK-242 pretreatment (Fig. 5C). With the correction of the rate of Ca^{2+} sparks, the SR Ca^{2+} content decreased by HMGB1 was largely restored by TAK-242 pretreatment (Figs. 5D, E). Concomitantly, TAK-242 pretreatment significantly increased the amplitude of AP-elicited Ca^{2+} transient and cell shortening impaired by HMGB1 treatment (Figs. 5F, G). TAK-242 restored the decreased Ca^{2+} transient and cell shortening by 56% and 61%, respectively.

It is well established that LPS can activate TLR4 signaling pathway [43]. We thus examined the effects of LPS on cardiac Ca^{2+} handling as a positive control. LPS (1 μg/ml) was added to cardiomyocytes for 30 min and induced an increase in the frequency of Ca^{2+} sparks,

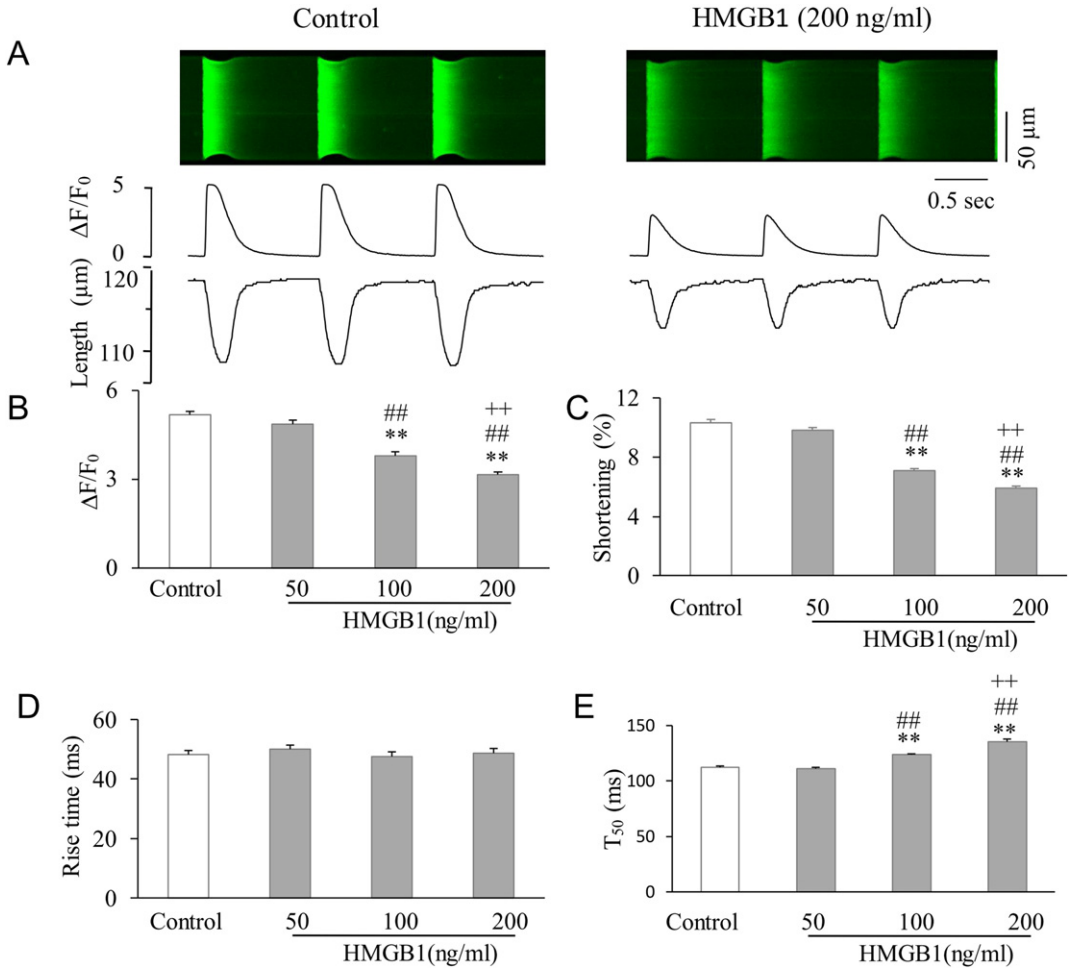

Fig. 3. HMGB1 impaired action potential-elicited Ca^{2+} transients and cellular contractility. A, representative line scan confocal measurement of Ca^{2+} transients and cellular contractility indexed by the cell shortening in cardiac myocytes from control and HMGB1 (200 ng/ml)-treated cells paced at 1 Hz. B, C, average of amplitude (ΔF / F0, B) and percentage (%) of maximum cell shortening (C). D, E, average of the rise time (D) and half-time of decay (T_{50}, E) of Ca^{2+} transients in control and different doses of HMGB1-treated cells. $^{**}p < 0.01$ vs. control; $^{\#\#}p < 0.01$ vs. 50 ng/ml HMGB1; $^{++}p < 0.01$ vs. 100 ng/ml HMGB1 (n = 89 to 188 cells in each group).

and decreases in SR Ca^{2+} content, Ca^{2+} transient and myocyte contractility (Fig. 5). TAK-242 (1 μM) largely inhibited LPS effects on Ca^{2+} handling. The results support the conclusion that activation of TLR4 signaling pathway induces SR Ca^{2+} leak and abnormal Ca^{2+} handling.

The role of TLR4 in HMGB1 effects on Ca^{2+} handling was further confirmed by knockdown of TLR4 with RNA interference (RNAi). Transfection of TLR4-shRNA in cultured NRVMs for 48 h resulted in 42% reduction of TLR4 protein compared with Ctrl-shRNA (Fig. 6A). HMGB1 produced similar effects on Ca^{2+} handling in NRVMs compared to those in adult cardiomyocytes. With TLR4 knockdown, the effect of HMGB1 on increasing the frequency of Ca^{2+} spark was inhibited (Fig. 6B). Meanwhile, the reduced SR Ca^{2+} content was restored by TLR4 knockdown (Fig. 6C). Concomitantly, the amplitude of Ca^{2+} transient was significantly increased (Fig. 6D). The results collectively implicate that TLR4 is responsible for HMGB1 regulation of Ca^{2+} handling in cardiomyocytes.

3.6. HMGB1 increased intracellular ROS production and RyR2 oxidation through TLR4

It has been suggested that HMGB1–TLR4 interaction induces intracellular ROS production by activation of NADPH oxidase [31,32]. Given that oxidative stress in RyR2 is an important reason for increasing RyR activity, we examined the oxidative status of RyR2. The results show that HMGB1 (200 ng/ml) significantly increased intracellular ROS production, as indicated by the increase of DCFDA fluorescence in ARVMs (Figs. 7A, B). Consistently, HMGB1 remarkably decreased mBB fluorescence of RyR2, indicating that the amount of free thiol groups in RyR2 is decreased (Figs. 7C, E). In contrast, HMGB1 had no effect on RyR2 protein levels (Fig. 7D). Antioxidant MnTBAP (100 μM) significantly inhibited the effects of HMGB1 on intracellular ROS production and RyR2 oxidation (Figs. 7A–E). Similar to the effect of MnTBAP, blocking TLR4 by pretreating the cells with TAK-242 for 30 min significantly inhibited HMGB1-induced intracellular ROS production and RyR2 oxidation (Figs. 7A–E). The results collectively indicate that HMGB1 increases intracellular ROS production and RyR2 oxidation through TLR4.

3.7. HMGB1 increased Ca^{2+}/calmodulin dependent protein kinase (CaMKII)-induced phosphorylation of RyR2

A recent study has demonstrated that intracellular ROS overproduction activated CaMKII by oxidizing the enzyme and consequently increased RyR2 activity by phosphorylation of the channel at Ser2814 [29]. We thus investigated whether HMGB1 increased CaMKII-induced phosphorylation of RyR2. The results show that

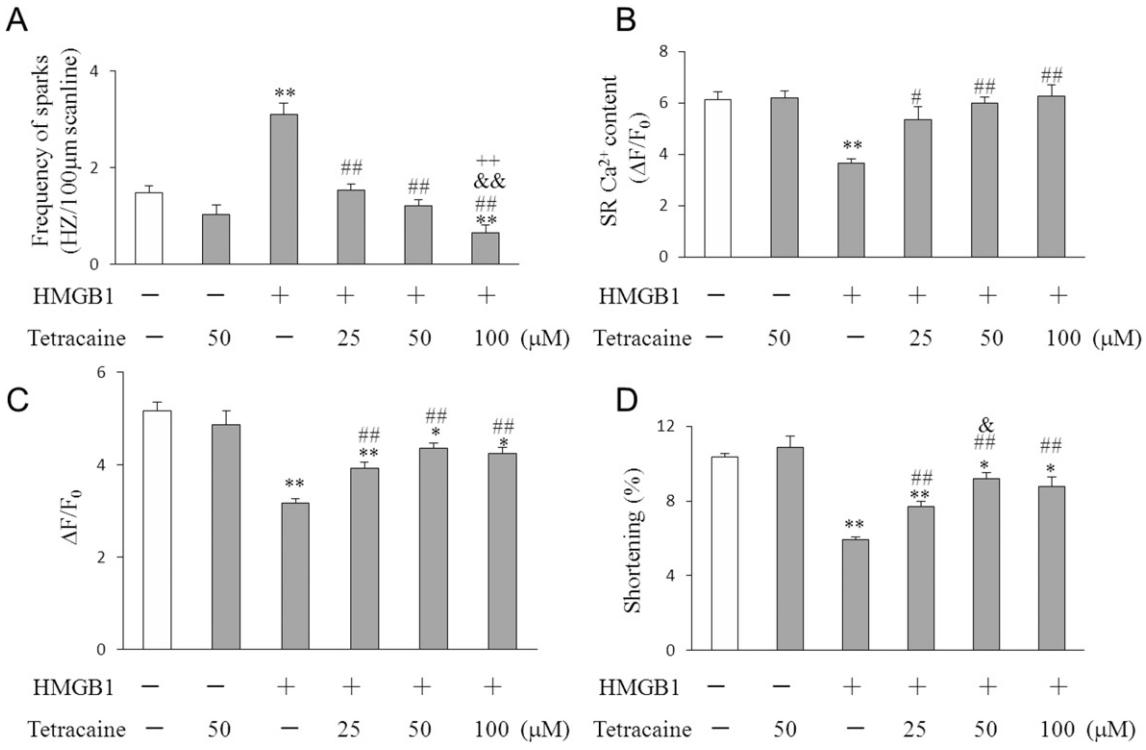

Fig. 4. Effects of tetracaine on HMGB1 modulation of Ca^{2+} handling and cellular contractility in cardiomyocytes. A–D, statistics of the frequency of Ca^{2+} sparks (n = 60 to 90 in each group, A), the amplitude of caffeine-elicited Ca^{2+} transient (n = 17 to 47, B), the amplitude of AP-elicited Ca^{2+} transient and maximum of cell shortening (n = 47 to 96, C, D) in control and HMGB1-treated groups without or with tetracaine pretreatment. $^{*}p < 0.05$, $^{**}p < 0.01$ vs. the value in HMGB1 (−) and tetracaine (−) group; $^{\#}p < 0.05$, $^{\#\#}p < 0.01$ vs. HMGB1 alone; $^{\&}p < 0.05$, $^{\&\&}p < 0.01$ vs. 25 μM tetracaine; $^{++}p < 0.01$ vs. 50 μM tetracaine.

HMGB1 increased CaMKII oxidation at methionine 281/282 (ox-CaMKII) without changing CaMKII protein expression (Fig. 8). Meanwhile, the phosphorylation of RyR2 at Ser2814 was increased by HMGB1 treatment (Fig. 8). Furthermore, blocking TLR4/ROS signaling with TAK-242 (1 μM) or MnTBAP (100 μM) inhibited the effects of HMGB1 on CaMKII oxidation and RyR2 phosphorylation (Fig. 8). The data indicate that HMGB1 increases phosphorylation of RyR2 at Ser2814 by activation of CaMKII through TLR4/ROS pathway.

3.8. Antioxidant MnTBAP normalized Ca^{2+} handling and myocyte contractility impaired by HMGB1

To test whether intracellular oxidative stress induced the hyperactive Ca^{2+} sparks, we explored the effect of antioxidant MnTBAP on the frequency of Ca^{2+} sparks upon HMGB1 stimulation. We found that HMGB1-induced high-frequent Ca^{2+} sparks were significantly inhibited by MnTBAP. With MnTBAP pretreatment, the effect of HMGB1 increasing the frequency of Ca^{2+} sparks was remarkably inhibited (Fig. 9A). Concomitantly, the SR Ca^{2+} content depleted by HMGB1 was restored (Fig. 9B). Meanwhile, MnTBAP significantly increased AP-elicited Ca^{2+} transient and cell shortening (Figs. 9C, D). With MnTBAP pretreatment, HMGB1-induced decreases of transient and cell shortening were increased by 84% and 56%, respectively. The data collectively implicate that the impairment of Ca^{2+} handling and EC coupling by HMGB1 is related to ROS production and RyR2 oxidation.

3.9. Effects of HMGB1 on L-type Ca^{2+} current ($I_{Ca,L}$)

Our previous study demonstrated that HMGB1 (200 ng/ml) decreased $I_{Ca,L}$ in neonatal rat ventricular myocytes [34]. In this study, we found that HMGB1 also significantly decreased $I_{Ca,L}$ at the voltages of −30−40 mV in adult rat ventricular myocytes ($p < 0.05$ at 0 and 30 mV, $p < 0.01$ at −10, 10 and 20 mV, Fig. 10). The peak $I_{Ca,L}$ (at 0 mV) was decreased by 40% by HMGB1 compared with the value in control. Neither TAK-242 (1 μM) nor MnTBAP (100 μM) had any significant effect on the magnitude of $I_{Ca,L}$. However, both TAK-242 and MnTBAP suppressed HMGB1-induced inhibition of $I_{Ca,L}$. TAK-242 and MnTBAP pretreatment inhibited the suppression effect of HMGB1 on peak $I_{Ca,L}$ (at 0 mV) by 38% and 25%, respectively.

4. Discussion

In this study, we demonstrated for the first time that HMGB1 impaired cardiac EC coupling by enhancing Ca^{2+} spark-mediated SR Ca^{2+} leak. The enhancement of SR Ca^{2+} leak caused partial depletion of SR Ca^{2+} content, which consequently decreased systolic Ca^{2+} transient and hence cardiac contractility. Furthermore, we revealed that oxidation and CaMKII-induced hyperphosphorylation of RyR2 (at Ser2814) underlie the hyperactive Ca^{2+} sparks upon HMGB1 stimulation. The intracellular oxidative stress was induced by HMGB1–TLR4 interaction. Inhibition of TLR4 or application of antioxidant prevented the enhancement of SR Ca^{2+} leak, resulting in improvement of cardiac EC coupling.

4.1. Enhancement of Ca^{2+} spark-mediated SR leak contributes to the impairment of cardiac EC coupling induced by HMGB1

There are two major Ca^{2+} sources contributing to intracellular Ca^{2+} transient which is essential to myocyte contraction upon cardiac excitation. One source is Ca^{2+} influx through L-type Ca^{2+} channels at the sarcolemmal membrane, which contributes to 10–30% of global

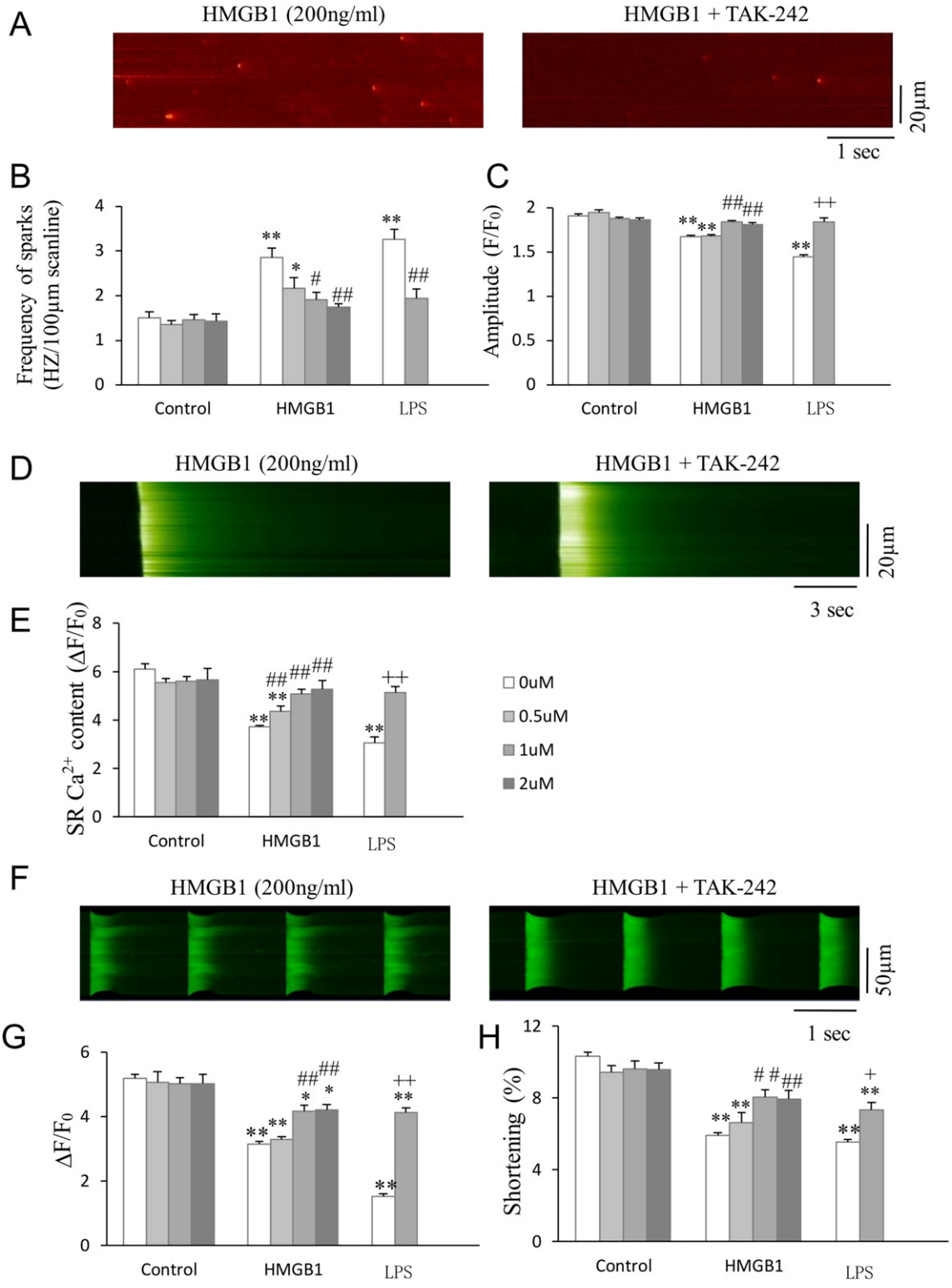

Fig. 5. Blocking TLR4 suppressed the effects of HMGB1 on Ca^{2+} handling and cellular contractility in cardiomyocytes. A, representative images of Ca^{2+} spark in HMGB1 (200 ng/ml)-treated cells without (left) or with (right) different doses of TAK-242 pretreatment. B, C, statistics of the frequency and amplitude of Ca^{2+} sparks in control, HMGB1- and LPS-treated cells without or with TAK-242 pretreatment (n = 20–61 cells in each group). D, representative images of caffeine-elicited Ca^{2+} transient in HMGB1-treated cells without (left) or with (right) TAK-242 pretreatment. E, statistics of the amplitude of SR Ca^{2+} content in control and HMGB1-treated cells without or with TAK-242 pretreatment (n = 44–63 cells in each group). F, representative images of AP-elicited Ca^{2+} transient in HMGB1-treated cells without (left) or with (right) TAK-242 pretreatment. G, H, statistics of the amplitude of Ca^{2+} transient (G) and the maximum of cell shortening (H, n = 19–75 in each group). $^{*}p < 0.05$, $^{**}p < 0.01$ vs. each respectively control; $^{\#}p < 0.05$, $^{\#\#}p < 0.01$ vs. HMGB1 without TAK-242 pretreatment; $^{+}p < 0.05$, $^{++}p < 0.01$ vs. LPS.

systolic Ca^{2+} transient and serves as a trigger of SR Ca^{2+} release through CICR mechanism. The other is the SR Ca^{2+} release, which accounts for the major part of the systolic Ca^{2+} transient [18,44]. SR Ca^{2+} content determines the amount of SR Ca^{2+} release, which in turn controls the amplitude of systolic Ca^{2+} transient and myocyte contractility. It is known that SR Ca^{2+} content is finely tuned by the SR Ca^{2+}

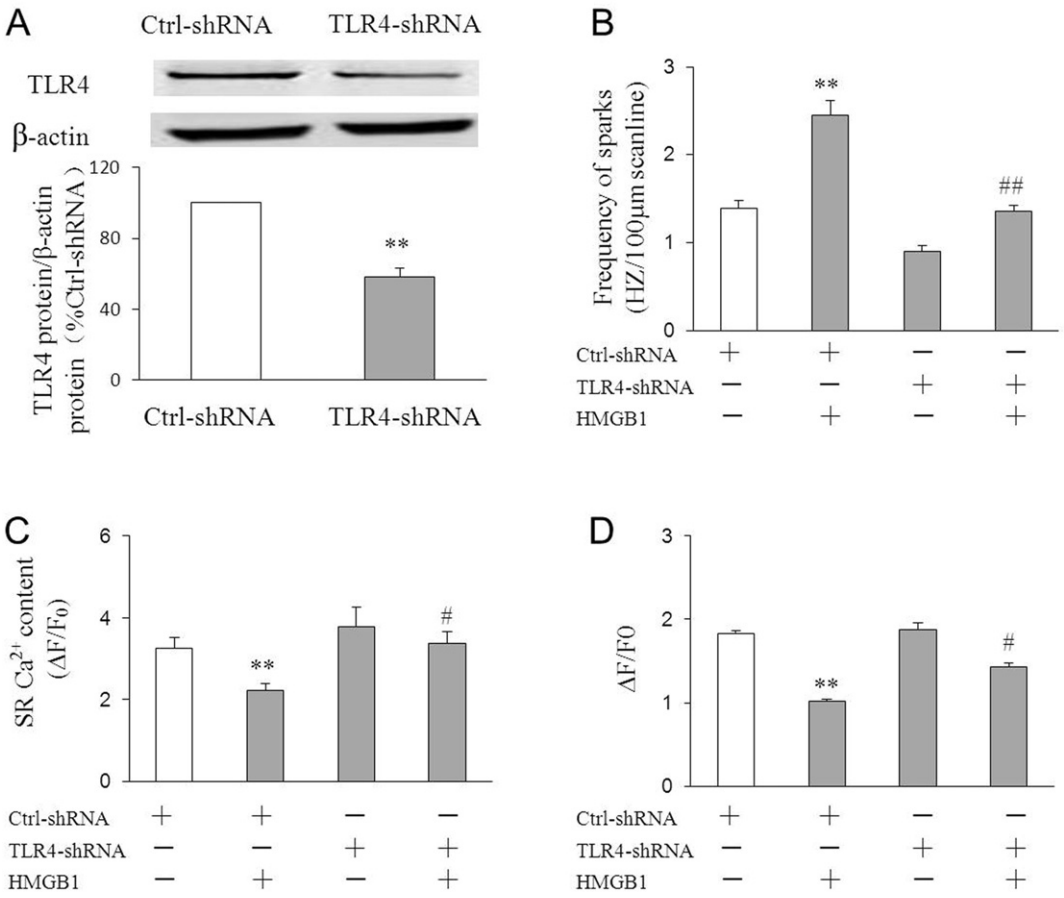

Fig. 6. Effects of down-regulating TLR4 expression on HMGB1 modulation of Ca^{2+} handling in neonatal cardiomyocytes. A, representative images of western blots of TLR4 and β-actin proteins and statistics of TLR4 abundance in Ctrl-shRNA and TLR4-shRNA groups (n = 4 in each group). B–D, statistics of the frequency of Ca^{2+} sparks (n = 60 to 72 in each group, B), the amplitude of caffeine-elicited Ca^{2+} transient (n = 35 to 50, C), and the amplitude of AP-elicited Ca^{2+} transient (n = 45 to 53, D) in Ctrl-shRNA and TLR4-shRNA groups with or without HMGB1 treatment. $^{**}p < 0.01$ vs. Ctrl-shRNA. $^{\#}p < 0.05$, $^{\#\#}p < 0.01$ vs. HMGB1 + Ctrl-shRNA.

release and SR Ca^{2+} recycling. Spontaneous Ca^{2+} sparks mediate diastolic SR Ca^{2+} leak, which is known to play an important role in setting the SR Ca^{2+} content at resting state [19,45]. Enhancement of SR Ca^{2+} leak across the SR has been observed in many heart diseases, including hypertrophy, heart failure, and burn-traumatized cardiac dysfunction. It causes reduction of diastolic SR Ca^{2+} content, leading to cardiac contractile dysfunction [21,46–48]. Furthermore, SR Ca^{2+} leak during diastole has been implicated in the initiation of Ca^{2+} waves which trigger various arrhythmias [23,24]. In this study, we found that HMGB1 dose-dependently enhanced Ca^{2+} spark-mediated SR leak. In parallel, SR Ca^{2+} content was reduced by HMGB1 in a dose-dependent manner. The data implicate the causal relationship between the increase of SR Ca^{2+} leak and reduction of SR Ca^{2+} content. Importantly, we found that prevention of the high-frequent Ca^{2+} sparks with RyR blocker, tetracaine, restored the reduced SR Ca^{2+} load, confirming that enhancement of SR Ca^{2+} leak is the major reason for the partial depletion of SR Ca^{2+} content upon HMGB1 stimulation. Consistent with the alteration of SR Ca^{2+} content, AP-elicited Ca^{2+} transient and myocyte contractility were dose-dependently decreased by HMGB1 treatment and were largely normalized by tetracaine pre-treatment. The effect of HMGB1 on RyR activity is quite like those of low concentrations of caffeine and ryanodine reported by Eisner's group [49]. It was demonstrated that both ryanodine (1–10 mM) and caffeine (0.5–10 mM) decreased the magnitude of the Ca^{2+} transient and reduced its rate of decay. The data are reproduced by a model in which caffeine and ryanodine decrease the magnitude of the Ca^{2+} transient by decreasing the Ca^{2+} content of the SR by increasing the leak of Ca^{2+} from the SR. This model is also applicable to HMGB1's effects, where HMGB1-induced enhancement of SR Ca^{2+} leak partially depletes the SR Ca^{2+} content, leading to a decrease of the amplitude of systolic Ca^{2+} transient and myocyte contractility.

Of note, HMGB1 slightly slowed systolic Ca^{2+} transient, suggesting that SERCA activity may be slightly reduced. There are also other possible explanations for this result. We found in our previous study that HMGB1 slightly prolonged action potential [34], which may contribute to the slightly slowed systolic Ca^{2+} transient. Furthermore, HMGB1-induced SR leak may also contribute to the slowed systolic Ca^{2+} transient because it has been suggested that if SR leak is sufficiently high, the SR will play no role in either Ca^{2+} release or re-uptake [47]. Recently, Eisner's group demonstrated that changes of SERCA activity have only modest effects on SR Ca^{2+} content in rat ventricular myocytes. In these considerations, SERCA has far less effect, if any, on HMGB1-induced partial depletion of SR load. Nevertheless, given to the important role of SERCA in Ca^{2+} handling and myocyte contractility, the effect of HMGB1 on SERCA activity and its contribution to HMGB1-induced cardiac dysfunction deserve future study.

There is a common sense that, in the steady state, the Ca^{2+} influx into the cell on each beat must equal the efflux of Ca^{2+}. Equally, the amount of Ca^{2+} released from the SR must equal that taken back up [50]. An increase in SR leak results in an increase of NCX activity and an increase in Ca^{2+} efflux, which will decrease the steady state SR Ca^{2+} content. Finally, enhanced SR leak sets a new balance between

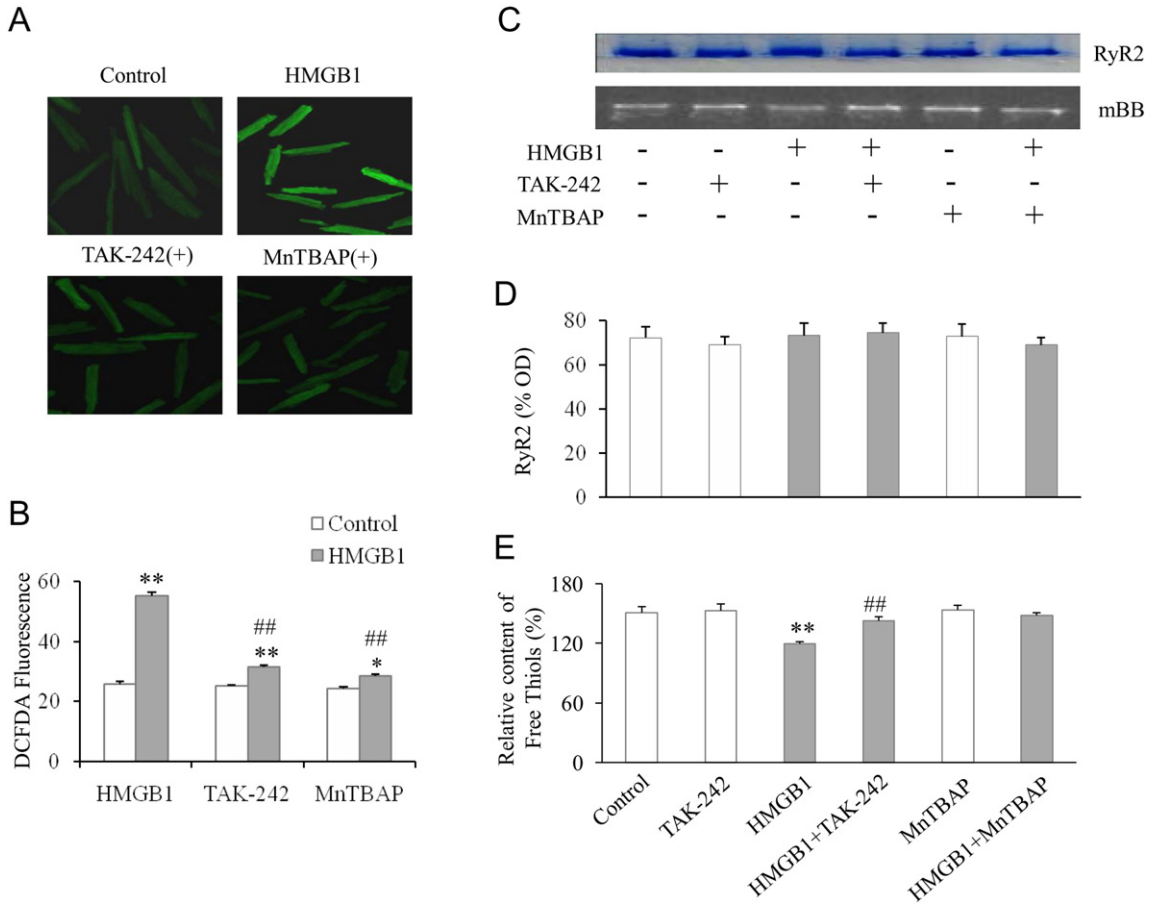

Fig. 7. HMGB1–TLR4 interaction increased intracellular ROS production and oxidative stress in RyR2 in cardiomyocytes. A, representative images of ROS-sensitive indicator DCFDA-loaded cells from control, HMGB1, HMGB1 + TAK-242 (TAK-242+) and HMGB1 + MnTBAP (MnTBAP+) groups. B, averages of DCFDA fluorescence in different groups. C, representative images of mBB fluorescence intensity and Coomassie-stained gels in parallel. D, E, statistics of RyR2 content (D) and relative free thiol content (%) of RyR2 (E) measured by normalizing mBB fluorescence to RyR2 level. $^{*}p < 0.05$, $^{**}p < 0.01$ vs. control; $^{\#\#}p < 0.01$ vs. HMGB1.

diastolic SR Ca^{2+} release and SR Ca^{2+} recycle under reduced SR Ca^{2+} content. At the new balance, Ca^{2+} influx required to maintain the leak might be attributed to (1) an increase in an unknown background Ca^{2+} influx during diastole; (2) Ca^{2+} entry on reverse NCX during systole; or (3) store-operated Ca^{2+} influx. In this study, we cannot distinguish the mechanism involved in the Ca^{2+} influx, which awaits future study.

Previous studies from other and our labs demonstrated that HMGB1 inhibited L-type Ca^{2+} current ($I_{Ca,L}$) in feline cardiomyocytes and in cultured neonatal rat cardiomyocytes [51]. In this study, we also found that HMGB1 (200 ng/ml) decreased the peak $I_{Ca,L}$ by 40% (at 0 mV, Fig. 10) in adult rat ventricular myocytes. This effect, as well as reduction of SR Ca^{2+} content, should contribute to HMGB1 induced decrease of Ca^{2+} transient. It has been suggested that there was a "redundancy" of trigger $I_{Ca,L}$ in a diad: reducing either the number of individual open channel or single channel current alone increased EC coupling gain [52,53]. Therefore, the decrease in $I_{Ca,L}$ causes a proportionately smaller decrease in Ca^{2+} transient. Our previous study showed that overexpression of Rad, a small G protein specifically inhibiting $Ca_v\beta$ function, decreased $I_{Ca,L}$ by 60%, while it only decreased the magnitude of Ca^{2+} transient by 42% [36]. In this study, 200 ng/ml HMGB1 decreased $I_{Ca,L}$ by 40% and SR Ca^{2+} content by 39%. Given to the complicated roles of both Ca^{2+} sources in the regulation of Ca^{2+} transient, we cannot tell exactly how much either SR leak-induced reduction of SR Ca^{2+} content or decrease in $I_{Ca,L}$ contributes to the decrease of Ca^{2+} transient upon HMGB1 stimulation. The data that restoration of SR Ca^{2+} content with tetracaine largely increased Ca^{2+} transient indicate that a decrease in SR Ca^{2+} content is an important reason for HMGB1-induced decrease of Ca^{2+} transient and impairment of myocyte contractility. Moreover, we found that blocking TLR4/ROS signaling with TAK-242 and MnTBAP had less suppression on $I_{Ca,L}$ (decreased by 38% and 25%, respectively) than on Ca^{2+} transient (decreased by 56% and 84%, respectively). The data further indicate that reduction in Ca^{2+} content is an important reason for HMGB1-induced negative inotropic effect.

4.2. TLR4–ROS signaling axis contributes to HMGB1 enhancement of SR Ca^{2+} leak

TLR4 is one of the major receptors for HMGB1-induced deleterious effects. HMGB1–TLR4 interaction has been suggested to participate in the pathogenesis of cardiac dysfunction by activating multiple signaling pathways [14,51,54–56]. For example, HMGB1 interacting with TLR4 induces cardiomyocyte apoptosis in cardiac I/R injury by potentiating TNF/JNK pathway [14]. It also promotes the development of diabetic cardiomyopathy by increasing IL-33 production [57]. Recently, Xu et al. show that HMGB1–TLR4 interaction results in inhibition of cardiac contractility [56]. Therefore, in this study we investigated the role of TLR4 in HMGB1-induced SR Ca^{2+} leak and the resulting impairment of cardiac EC coupling. We found that blocking TLR4 with its specific inhibitor TAK-242 or knockdown of TLR4 by RNAi significantly inhibited HMGB1-induced SR Ca^{2+} leak, largely restored the partially depleted SR Ca^{2+} content and

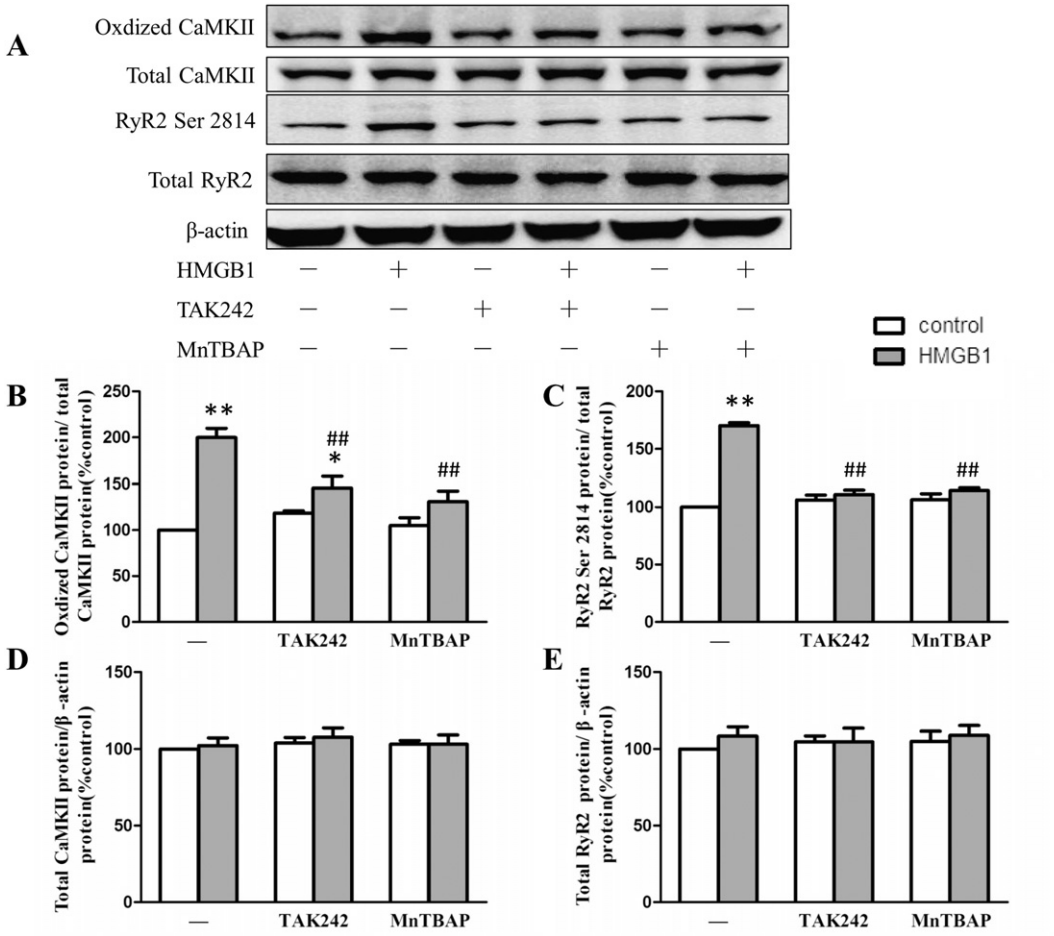

Fig. 8. HMGB1 activated CaMKII and increased RyR2 phosphorylation at Ser2814 in cardiomyocytes. A, representative western blots of proteins of oxidized CaMKII (at methionine 281/282) and total CaMKII, phosphorylated RyR2 (at Ser2814) and total RyR2, and β-actin from cardiomyocytes in control and HMGB1-treated group without (−) or with TAK-242/MnTBAP treatment. B, C, statistics of protein levels of oxidized CaMKII (B) and phosphorylated RyR2 (C) normalized by protein levels of total CaMKII or RyR2. D, E, statistics of protein levels of total CaMKII (D) and RyR2 (E). $^{*}p < 0.05$, $^{**}p < 0.01$ vs. each respective control; $^{\#\#}p < 0.01$ vs. HMGB1 in (−) group. n = 4 in each group.

remarkably increased the compromised Ca^{2+} transient and myocyte contractility. The data indicate that TLR4 is an important molecule responsible for transducing HMGB1 signaling on Ca^{2+} handling and EC coupling in cardiomyocytes.

TLR4 signaling transduction is linked to ROS overproduction by activation of NAD(P)H oxidase and other signaling pathways [31,32,58]. HMGB1–TLR4 interaction is demonstrated to activate NAD(P)H oxidase in neutrophils to promote hemorrhagic shock through increasing ROS production [31]. TLR4 is highly expressed in cardiac myocytes and activation of TLR4–ROS signaling pathway has been suggested to induce cardiac apoptosis [59]. In this study, we found that HMGB1 induced intracellular ROS overproduction, which could be largely inhibited by blocking TLR4 with TAK-242. The increase in intracellular ROS production induced oxidative stress in RyR2 and phosphorylation of RyR2 at Ser2814 by activation of CaMKII. Antioxidant MnTBAP suppressed oxidative stress and CaMKII-induced phosphorylation in RyR2 in HMGB1 treated cells and consequently suppressed high-frequent Ca^{2+} sparks in cardiomyocytes. Accordingly, MnTBAP restored SR Ca^{2+} content and remarkably increased systolic Ca^{2+} transient and myocyte contractility. The data collectively indicate that TLR4–ROS signaling axis contributes to HMGB1-induced SR Ca^{2+} leak and the consequent abnormal regulation of EC coupling in cardiomyocytes.

4.3. Implications

HMGB1 has been suggested to participate in the pathogenesis of cardiac dysfunction in many diseases, such as myocardial infarction [60], cardiac I/R injury [6], diabetic cardiomyopathy [8], septic cardiac dysfunction [7], and trauma-induced cardiac dysfunction [61]. The concentrations of HMGB1 applied in this study are comparable to the pathological HMGB1 concentrations in serum in sepsis and trauma [7,61], as well as in heart tissue in myocardial infarction and I/R injury as discussed in our previous study [34]. Here we revealed for the first time that HMGB1 impaired cardiac contractile function by inducing SR Ca^{2+} leak. In cardiac I/R injury, as well as burn-generated cardiac dysfunction, SR Ca^{2+} leak has been suggested to be an important reason for the pathogenesis of contractile dysfunction. The present findings suggest that HMGB1 accounts, at least partially, for the SR Ca^{2+} leak in these heart diseases. Although no study investigates whether SR leak presents and participates in the pathogenesis of septic cardiac dysfunction and diabetic cardiomyopathy, the important role of HMGB1 in these diseases suggests that SR Ca^{2+} leak may be an important mechanism for the development of cardiac dysfunction in sepsis and diabetic cardiomyopathy. In this consideration, anti-SR Ca^{2+} leak may be a potential therapeutic strategy for the treatment of septic cardiac dysfunction and diabetic cardiomyopathy.

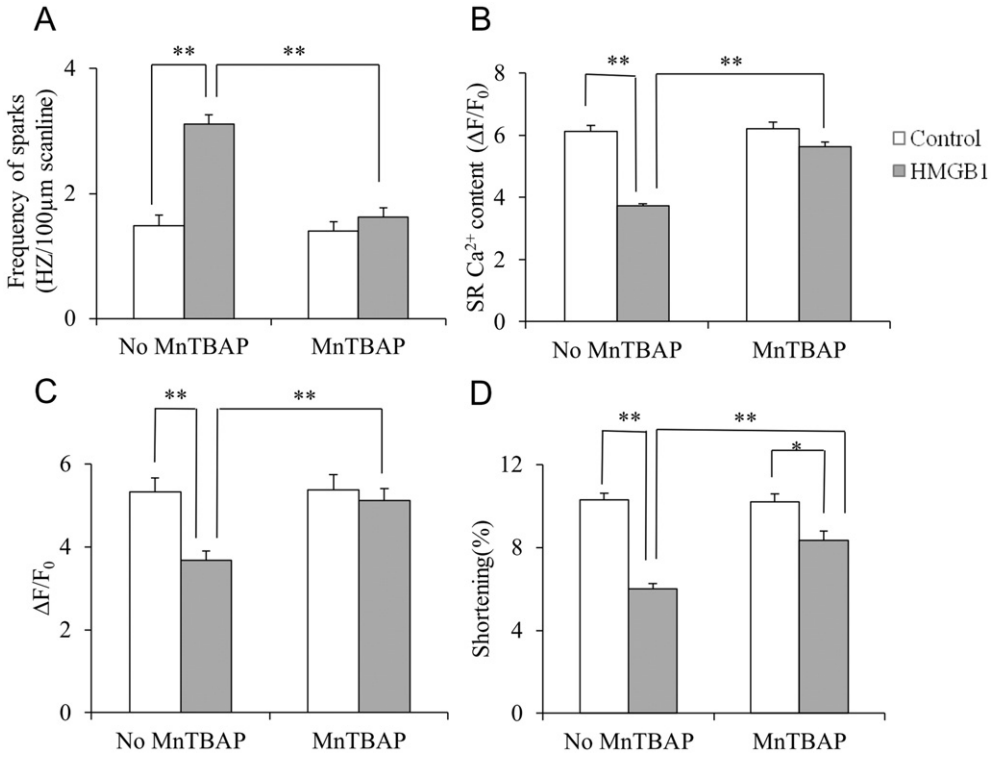

Fig. 9. Antioxidant MnTBAP normalized the impairment of Ca^{2+} handling and myocyte contractility induced by HMGB1. A–D, statistics of the frequency of Ca^{2+} sparks (n = 45 to 85 in each group, A), the amplitude of caffeine-elicited Ca^{2+} transient (n = 48 to 56, B), the amplitude of AP-elicited Ca^{2+} transient and maximum of cell shortening (%, n = 55 to 64, C, D) in control and HMGB1-treated groups without or with MnTBAP pretreatment. $^{*}p < 0.05$, $^{**}p < 0.01$.

There is currently a disagreement regarding the role of HMGB1 in the development of ischemic heart diseases; some studies suggest that it is beneficial by inducing myocardial regeneration and improving cardiac dysfunction and remodeling after MI [11], whereas others implicate that it is deleterious by causing an increase in the inflammatory responses and worsens the cardiac dysfunction and remodeling after myocardial ischemia–reperfusion injury [6]. The discrepancy has been suggested to be related to the dosage of HMGB1 applied, where HMGB1 administration is beneficial in low doses and detrimental in high doses [62]. In this study, we found that HMGB1 induced significant SR Ca^{2+} leak and reduction of SR Ca^{2+} content only at relatively high doses (≥100 ng/ml). The data support the notion and provide implication for safe manipulation of HMGB1 in the treatment of ischemic heart diseases.

In summary, this study reveals for the first time that HMGB1 causes SR Ca^{2+} leak and the consequent impairment of EC coupling through TLR4–ROS signaling in cardiomyocytes. The present finding implicates that anti-SR Ca^{2+} leak may be a potential therapeutic strategy for the treatment of cardiac dysfunction related to HMGB1 overproduction.

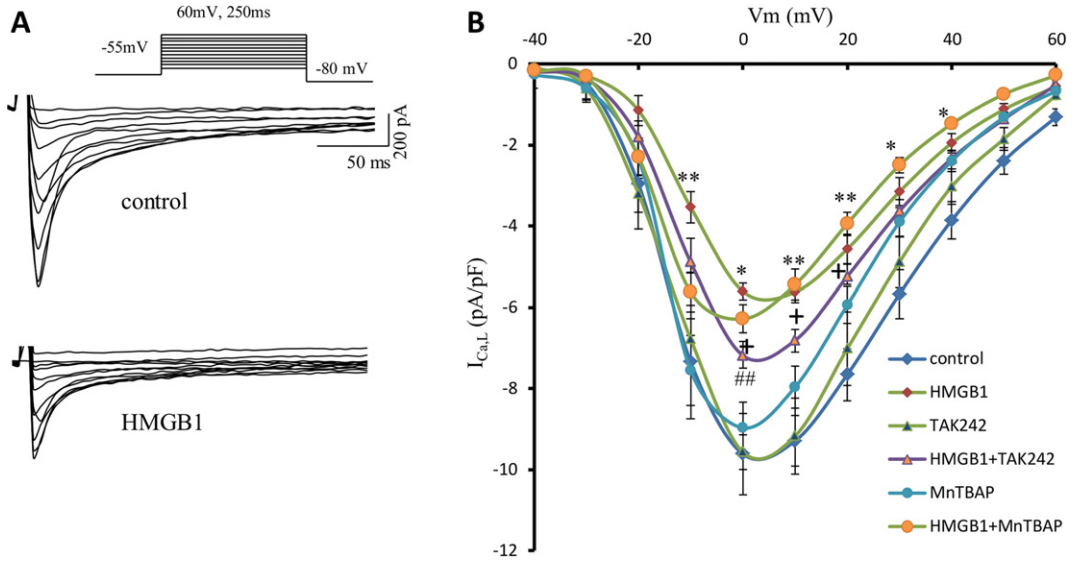

Fig. 10. HMGB1 decreased $I_{Ca,L}$ in adult rat ventricular myocytes. A, representative whole-cell $I_{Ca,L}$ in control and HMGB1-treated cells. B, average $I_{Ca,L}$ density–voltage (*I–V*) relationships. $^{*}p < 0.05$, $^{**}p < 0.01$ vs. control; $^{\#\#}p < 0.01$ vs. TAK-242; $^{+}p < 0.05$ vs. MnTBAP. n = 9–12 in each group.

Conflict of interest statement

None.

Acknowledgments

This work was supported by the National Natural Science Foundation of China (Nos. 31171096, 31371159 and 81200122) and Basic Research Foundation of Shenzhen (Nos. JC201005250059A, JCYJ20120613115535998 and JCYJ20130326112207234).

References

[1] Neumann FJ, Ott I, Gawaz M, Richardt G, Holzapfel H, Jochum M, et al. Cardiac release of cytokines and inflammatory responses in acute myocardial infarction. Circulation 1995;92:748–55.
[2] Suleiman M, Khatib R, Agmon Y, Mahamid R, Boulos M, Kapeliovich M, et al. Early inflammation and risk of long-term development of heart failure and mortality in survivors of acute myocardial infarction predictive role of C-reactive protein. J Am Coll Cardiol 2006;47:962–8.
[3] Kobara M, Noda K, Kitamura M, Okamoto A, Shiraishi T, Toba H, et al. Antibody against interleukin-6 receptor attenuates left ventricular remodelling after myocardial infarction in mice. Cardiovasc Res 2010;87:424–30.
[4] Nishikawa K, Yoshida M, Kusuhara M, Ishigami N, Isoda K, Miyazaki K, et al. Left ventricular hypertrophy in mice with a cardiac-specific overexpression of interleukin-1. Am J Physiol Heart Circ Physiol 2006;291:H176–83.
[5] Yang Z, Zingarelli B, Szabo C. Crucial role of endogenous interleukin-10 production in myocardial ischemia/reperfusion injury. Circulation 2000;101:1019–26.
[6] Andrassy M, Volz HC, Igwe JC, Funke B, Eichberger SN, Kaya Z, et al. High-mobility group box-1 in ischemia–reperfusion injury of the heart. Circulation 2008;117:3216–26.
[7] Sunden-Cullberg J, Norrby-Teglund A, Rouhiainen A, Rauvala H, Herman G, Tracey KJ, et al. Persistent elevation of high mobility group box-1 protein (HMGB1) in patients with severe sepsis and septic shock. Crit Care Med 2005;33:564–73.
[8] Volz HC, Seidel C, Laohachewin D, Kaya Z, Muller OJ, Pleger ST, et al. HMGB1: the missing link between diabetes mellitus and heart failure. Basic Res Cardiol 2010;105:805–20.
[9] Wang H, Yang H, Tracey KJ. Extracellular role of HMGB1 in inflammation and sepsis. J Intern Med 2004;255:320–31.
[10] Yang H, Wang H, Czura CJ, Tracey KJ. The cytokine activity of HMGB1. J Leukoc Biol 2005;78:1–8.
[11] Kohno T, Anzai T, Naito K, Miyasho T, Okamoto M, Yokota H, et al. Role of high-mobility group box 1 protein in post-infarction healing process and left ventricular remodelling. Cardiovasc Res 2009;81:565–73.
[12] Wang H, Bloom O, Zhang M, Vishnubhakat JM, Ombrellino M, Che J, et al. HMG-1 as a late mediator of endotoxin lethality in mice. Science 1999;285:248–51.
[13] Wang LJ, Lu L, Zhang FR, Chen QJ, De Caterina R, Shen WF. Increased serum high-mobility group box-1 and cleaved receptor for advanced glycation endproducts levels and decreased endogenous secretory receptor for advanced glycation endproducts levels in diabetic and non-diabetic patients with heart failure. Eur J Heart Fail 2011;13:440–9.
[14] Xu H, Yao Y, Su Z, Yang Y, Kao R, Martin CM, et al. Endogenous HMGB1 contributes to ischemia–reperfusion-induced myocardial apoptosis by potentiating the effect of TNF-α/JNK. Am J Physiol Heart Circ Physiol 2011;300:H913–21.
[15] Qin S, Wang H, Yuan R, Li H, Ochani M, Ochani K, et al. Role of HMGB1 in apoptosis-mediated sepsis lethality. J Exp Med 2006;203:1637–42.
[16] Limana F, Germani A, Zacheo A, Kajstura J, Di Carlo A, Borsellino G, et al. Exogenous high-mobility group box 1 protein induces myocardial regeneration after infarction via enhanced cardiac C-kit$^+$ cell proliferation and differentiation. Circ Res 2005;97:e73–83.
[17] Cheng H, Wang SQ. Calcium signaling between sarcolemmal calcium channels and ryanodine receptors in heart cells. Front Biosci 2002;7:d1867–78.
[18] Bers DM. Cardiac excitation–contraction coupling. Nature 2002;415:198–205.
[19] Lukyanenko V, Viatchenko-Karpinski S, Smirnov A, Wiesner TF, Gyorke S. Dynamic regulation of sarcoplasmic reticulum Ca^{2+} content and release by luminal Ca^{2+}-sensitive leak in rat ventricular myocytes. Biophys J 2001;81:785–98.
[20] Terentyev D, Gyorke I, Belevych AE, Terentyeva R, Sridhar A, Nishijima Y, et al. Redox modification of ryanodine receptors contributes to sarcoplasmic reticulum Ca^{2+} leak in chronic heart failure. Circ Res 2008;103:1466–72.
[21] Deng J, Wang G, Huang Q, Yan Y, Li K, Tan W, et al. Oxidative stress-induced leaky sarcoplasmic reticulum underlying acute heart failure in severe burn trauma. Free Radic Biol Med 2008;44:375–85.
[22] Kubalova Z, Terentyev D, Viatchenko-Karpinski S, Nishijima Y, Gyorke I, Terentyeva R, et al. Abnormal intrastore calcium signaling in chronic heart failure. Proc Natl Acad Sci U S A 2005;102:14104–9.
[23] Lyon AR, Bannister ML, Collins T, Pearce E, Sepehripour AH, Dubb SS, et al. SERCA2a gene transfer decreases sarcoplasmic reticulum calcium leak and reduces ventricular arrhythmias in a model of chronic heart failure. Circ Arrhythm Electrophysiol 2011;4:362–72.
[24] Shan J, Xie W, Betzenhauser M, Reiken S, Chen BX, Wronska A, et al. Calcium leak through ryanodine receptors leads to atrial fibrillation in 3 mouse models of catecholaminergic polymorphic ventricular tachycardia. Circ Res 2012;111:708–17.
[25] Yano M, Okuda S, Oda T, Tokuhisa T, Tateishi H, Mochizuki M, et al. Correction of defective interdomain interaction within ryanodine receptor by antioxidant is a new therapeutic strategy against heart failure. Circulation 2005;112:3633–43.
[26] Duncan DJ, Yang Z, Hopkins PM, Steele DS, Harrison SM. TNF-alpha and IL-1beta increase Ca^{2+} leak from the sarcoplasmic reticulum and susceptibility to arrhythmia in rat ventricular myocytes. Cell Calcium 2010;47:378–86.
[27] Hidalgo C, Donoso P, Carrasco MA. The ryanodine receptors Ca^{2+} release channels: cellular redox sensors? IUBMB Life 2005;57:315–22.
[28] Pessah IN, Kim KH, Feng W. Redox sensing properties of the ryanodine receptor complex. Front Biol 2002;7:a72–9.
[29] Ho HT, Liu B, Snyder JS, Lou Q, Brundage EA, Velez-Cortes F, et al. Ryanodine receptor phosphorylation by oxidized CaMKII contributes to the cardiotoxic effects of cardiac glycosides. Cardiovasc Res 2014;101:165–74.
[30] Sag CM, Kohler AC, Anderson ME, Backs J, Maier LS. CaMKII-dependent SR Ca leak contributes to doxorubicin-induced impaired Ca handling in isolated cardiac myocytes. J Mol Cell Cardiol 2011;51:749–59.
[31] Fan J, Li Y, Levy RM, Fan JJ, Hackam DJ, Vodovotz Y, et al. Hemorrhagic shock induces NAD(P)H oxidase activation in neutrophils: role of HMGB1–TLR4 signaling. J Immunol 2007;178:6573–80.
[32] Tsung A, Klune JR, Zhang X, Jeyabalan G, Cao Z, Peng X, et al. HMGB1 release induced by liver ischemia involves Toll-like receptor 4 dependent reactive oxygen species production and calcium-mediated signaling. J Exp Med 2007;204:2913–23.
[33] Deng J, Liu W, Wang Y, Dong M, Zheng M, Liu J. Polydatin modulates Ca^{2+} handling, excitation–contraction coupling and beta-adrenergic signaling in rat ventricular myocytes. J Mol Cell Cardiol 2012;53:646–56.
[34] Liu W, Deng J, Xu J, Wang H, Yuan M, Liu N, et al. High-mobility group box 1 (HMGB1) downregulates cardiac transient outward potassium current (I_{to}) through downregulation of Kv4.2 and Kv4.3 channel transcripts and proteins. J Mol Cell Cardiol 2010;49:438–48.
[35] Jiang X, Liu W, Deng J, Lan L, Xue X, Zhang C, et al. Polydatin protects cardiac function against burn injury by inhibiting sarcoplasmic reticulum Ca leak by reducing oxidative modification of ryanodine receptors. Free Radic Biol Med 2013;60:292–9.
[36] Wang G, Zhu X, Xie W, Han P, Li K, Sun Z, et al. Rad as a novel regulator of excitation–contraction coupling and beta-adrenergic signaling in heart. Circ Res 2010;106:317–27.
[37] Cheng H, Song LS, Shirokova N, Gonzalez A, Lakatta EG, Rios E, et al. Amplitude distribution of calcium sparks in confocal images: theory and studies with an automatic detection method. Biophys J 1999;76:606–17.
[38] Venetucci LA, Trafford AW, Diaz ME, O'Neill SC, Eisner DA. Reducing ryanodine receptor open probability as a means to abolish spontaneous Ca^{2+} release and increase Ca^{2+} transient amplitude in adult ventricular myocytes. Circ Res 2006;98:1299–305.
[39] Ramay HR, Liu OZ, Sobie EA. Recovery of cardiac calcium release is controlled by sarcoplasmic reticulum refilling and ryanodine receptor sensitivity. Cardiovasc Res 2011;91:598–605.
[40] Overend CL, O'Neill SC, Eisner DA. The effect of tetracaine on stimulated contractions, sarcoplasmic reticulum Ca^{2+} content and membrane current in isolated rat ventricular myocytes. J Physiol 1998;507(Pt 3):759–69.
[41] van Beijnum JR, Buurman WA, Griffioen AW. Convergence and amplification of toll-like receptor (TLR) and receptor for advanced glycation end products (RAGE) signaling pathways via high mobility group B1 (HMGB1). Angiogenesis 2008;11:91–9.
[42] Zong M, Bruton JD, Grundtman C, Yang H, Li JH, Alexanderson H, et al. TLR4 as receptor for HMGB1 induced muscle dysfunction in myositis. Ann Rheum Dis 2013;72:1390–9.
[43] Lee IT, Shih RH, Lin CC, Chen JT, Yang CM. Role of TLR4/NADPH oxidase/ROS-activated p38 MAPK in VCAM-1 expression induced by lipopolysaccharide in human renal mesangial cells. Cell Commun Signal 2012;10:33.
[44] Cheng H, Lederer WJ. Calcium sparks. Physiol Rev 2008;88:1491–545.
[45] Shannon TR, Ginsburg KS, Bers DM. Quantitative assessment of the SR Ca^{2+} leak–load relationship. Circ Res 2002;91:594–600.
[46] Gomez AM, Valdivia HH, Cheng H, Lederer MR, Santana LF, Cannell MB, et al. Defective excitation–contraction coupling in experimental cardiac hypertrophy and heart failure. Science 1997;276:800–6.
[47] Hobai IA, O'Rourke B. Decreased sarcoplasmic reticulum calcium content is responsible for defective excitation–contraction coupling in canine heart failure. Circulation 2001;103:1577–84.
[48] White DJ, Maass DL, Sanders B, Horton JW. Cardiomyocyte intracellular calcium and cardiac dysfunction after burn trauma. Crit Care Med 2002;30:14–22.
[49] Negretti N, O'Neill SC, Eisner DA. The effects of inhibitors of sarcoplasmic reticulum function on the systolic Ca^{2+} transient in rat ventricular myocytes. J Physiol 1993;468:35–52.
[50] Eisner D, Bode E, Venetucci L, Trafford A. Calcium flux balance in the heart. J Mol Cell Cardiol 2013;58:110–7.
[51] Tzeng HP, Fan J, Vallejo JG, Dong JW, Chen X, Houser SR, et al. Negative inotropic effects of high-mobility group box 1 protein in isolated contracting cardiac myocytes. Am J Physiol Heart Circ Physiol 2008;294:H1490–6.
[52] Altamirano J, Bers DM. Voltage dependence of cardiac excitation–contraction coupling: unitary Ca^{2+} current amplitude and open channel probability. Circ Res 2007;101:590–7.

[53] Polakova E, Zahradnikova Jr A, Pavelkova J, Zahradnik I, Zahradnikova A. Local calcium release activation by DHPR calcium channel openings in rat cardiac myocytes. J Physiol 2008;586:3839–54.
[54] Sachdev U, Cui X, Tzeng E. HMGB1 and TLR4 mediate skeletal muscle recovery in a murine model of hindlimb ischemia. J Vasc Surg 2013;58:460–9.
[55] Yao Y, Xu X, Zhang G, Zhang Y, Qian W, Rui T. Role of HMGB1 in doxorubicin-induced myocardial apoptosis and its regulation pathway. Basic Res Cardiol 2012;107:267.
[56] Xu H, Su Z, Wu J, Yang M, Penninger JM, Martin CM, et al. The alarmin cytokine, high mobility group box 1, is produced by viable cardiomyocytes and mediates the lipopolysaccharide-induced myocardial dysfunction via a TLR4/phosphatidylinositol 3-kinase gamma pathway. J Immunol 2010;184:1492–8.
[57] Arshad MI, Piquet-Pellorce C, Samson M. IL-33 and HMGB1 alarmins: sensors of cellular death and their involvement in liver pathology. Liver Int 2012;32:1200–10.
[58] Kampfrath T, Maiseyeu A, Ying Z, Shah Z, Deiuliis JA, Xu X, et al. Chronic fine particulate matter exposure induces systemic vascular dysfunction via NADPH oxidase and TLR4 pathways. Circ Res 2011;108:716–26.
[59] Zhang Y, Peng T, Zhu H, Zheng X, Zhang X, Jiang N, et al. Prevention of hyperglycemia-induced myocardial apoptosis by gene silencing of Toll-like receptor-4. J Transl Med 2010;8:133.
[60] He YY, Wen Y, Zheng XX, Jiang XJ. Intramyocardial delivery of HMGB1 by a novel thermosensitive hydrogel attenuates cardiac remodeling and improves cardiac function after myocardial infarction. J Cardiovasc Pharmacol 2013;61:283–90.
[61] Levy RM, Mollen KP, Prince JM, Kaczorowski DJ, Vallabhaneni R, Liu S, et al. Systemic inflammation and remote organ injury following trauma require HMGB1. Am J Physiol Regul Integr Comp Physiol 2007;293:R1538–44.
[62] Lotze MT, Tracey KJ. High-mobility group box 1 protein (HMGB1): nuclear weapon in the immune arsenal. Nat Rev Immunol 2005;5:331–42.